

# LISA, PTA and $\gamma$ -ray telescopes as multi-messenger probes of a cosmological first-order phase transition and intergalactic magnetic fields



Cosmology in the Alps 2024  
Mar. 18, 2024



Alberto Roper Pol  
*University of Geneva*

SNSF Ambizione grant: “*Exploring the early universe with gravitational waves  
and primordial magnetic fields*”

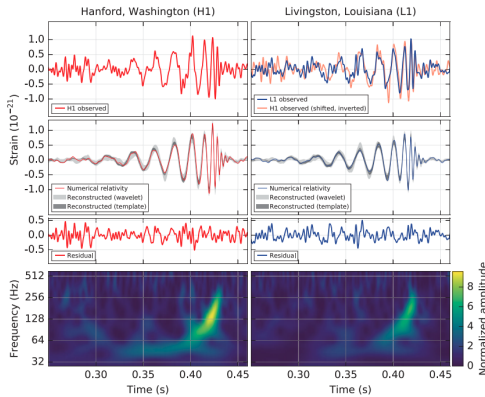
*Collaborators:* A. Brandenburg (Nordita), T. Boyer (APC), C. Caprini  
(UniGe/CERN), T. Kahniashvili (CMU), A. Kosowsky (PittU), S. Mandal  
(CMU), A. Neronov (APC/EPFL), S. Procacci (UniGe), D. Semikoz (APC)

arXiv: 1903.08585, 2009.14174, 2201.05630, 2307.10744, 2403.03723

<https://github.com/AlbertoRoper/cosmoGW> [CosmoGW]

# Introduction and Motivation

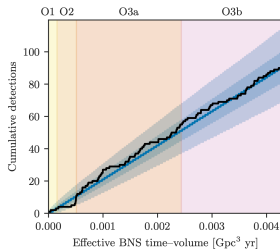
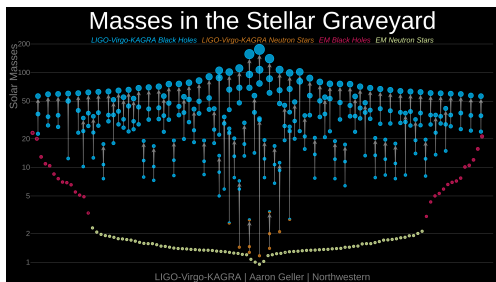
- Gravitational waves are opening a new window into our understanding of the Universe
  - First event GW150914 detected<sup>1</sup>



<sup>1</sup>[LIGO-Virgo Collaboration], *Phys. Rev. Lett.* **116**, 061102 (2016)

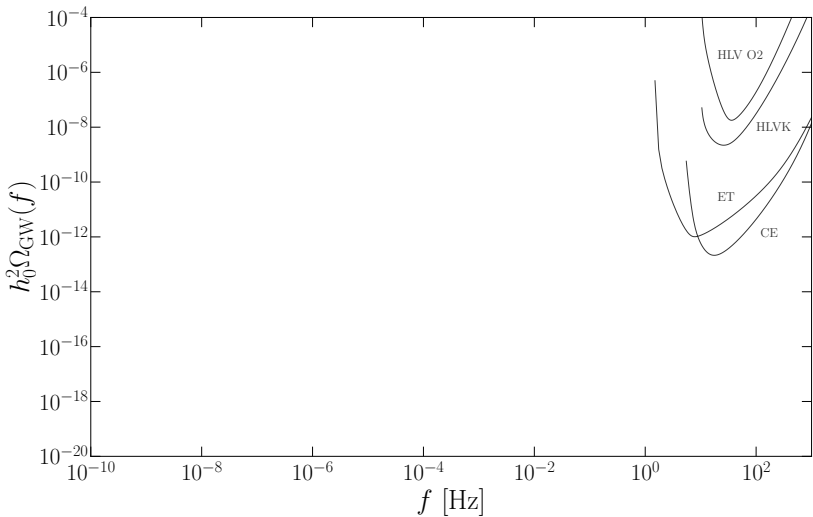
# Introduction and Motivation

- GW170817 NS binary merger: first detection of GW and EM counterpart (constraint on the GW speed, measure of the Hubble rate)
- Several following events: LIGO-Virgo-KAGRA started the fourth observing run (O4) in May 2023 → 90 events up to O3b<sup>2</sup>



<sup>2</sup>[LIGO-Virgo Collaboration], GWTC-3, arXiv:2111.03606 (2021).

## Gravitational spectrum (ground-based detectors)



## LISA

- Laser Interferometer Space Antenna (LISA) is a space-based interferometer
- Approved in 2017 as one of the main research missions of ESA (L3) with NASA collaboration
- Mission adoption phase in January 2024
- Launch planned for 2034
- Composed by three spacecrafts in a distance of 2.5M km

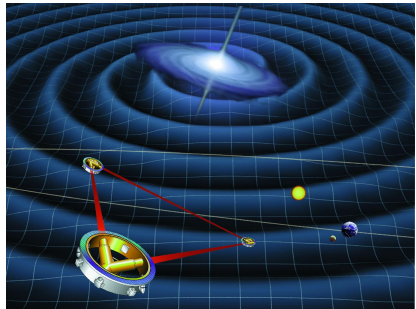
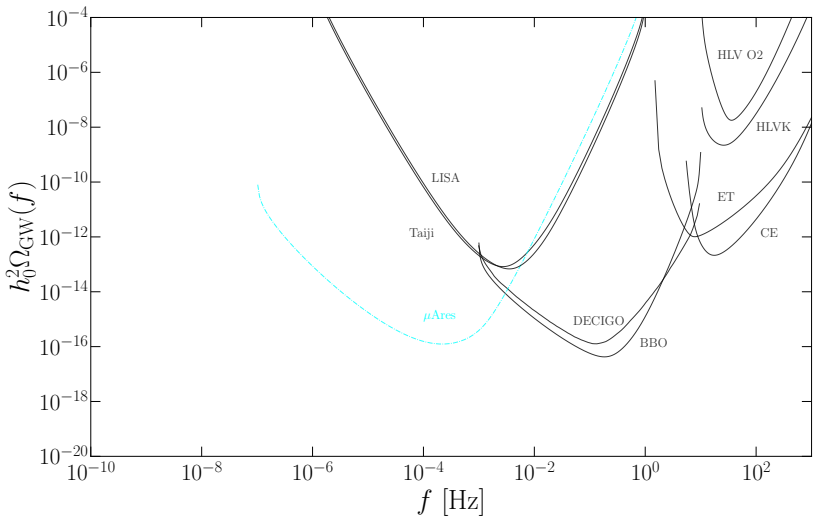


Figure: Artist's impression of LISA from Wikipedia

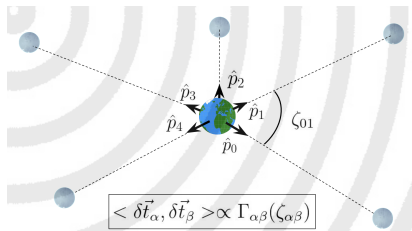
## Gravitational spectrum (space-based detectors)



## Pulsar Timing Array (PTA)

- An array of millisecond pulsars (MSP) is observed in the radio band to compute the delays on the time of arrival due to the presence of GWs.
- Collected data is the time series of residuals for each pulsar:

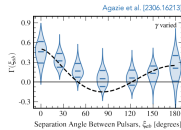
$$\delta t^i = t_{\text{obs}}^i - t_{\text{TM}}^i$$



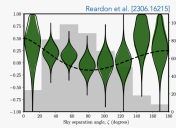
# PTA detection

- The PTA collaborations reported for the first-time evidence of a stochastic gravitational wave background on a press release on June 28, 2023 (plus a series of papers by each collaboration).

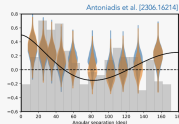
NANOGrav:  
68 pulsars, 16yr of data  
 $\sim 3\sigma$  significance



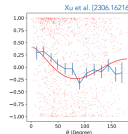
PPTA:  
32 pulsars, 18yr of data  
 $\sim 2\sigma$  significance



EPTA + InPTA:  
25 pulsars, 24yr of data  
 $\sim 3\sigma$  significance



CPTA:  
57 pulsars, 3yr of data  
 $\sim 4.6\sigma$  significance



Credit: Andrea Mitridate

# Cosmological GWs

Main considered source of the signal is from the superposition of supermassive black hole binaries (SMBHB), but other sources are also possible: individual sources<sup>4</sup> or early universe sources<sup>5</sup> (cosmological GW background).

Cosmological GWs have the potential to provide us with *direct information on early universe physics* that is *not directly accessible via electromagnetic observations, possibly complementary to collider experiments*:

nature of first-order phase transitions (baryogenesis, BSM physics, high-energy physics),

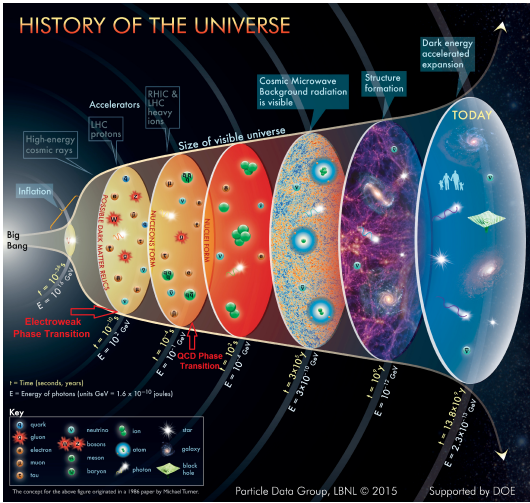
*primordial origin of intergalactic magnetic fields.*

---

<sup>4</sup> [EPTA Collaboration], *The second data release from the European Pulsar Timing Array IV: Search for continuous gravitational wave signals*, arXiv:2306.16226

<sup>5</sup> [EPTA Collaboration] (incl. ARP), *The second data release from the European Pulsar Timing Array: V. Implications for massive black holes, dark matter and the early Universe*, arXiv:2306.16227.  
[NANOGrav Collaboration], *The NANOGrav 15 yr Data Set: Search for Signals from New Physics*, arXiv:2306.16219.

# HISTORY OF THE UNIVERSE



# Probing the early Universe with GWs

## Cosmological (pre-recombination) GW background

- Why background? Individual sources are not resolvable, superposition of single events occurring in the whole Universe.

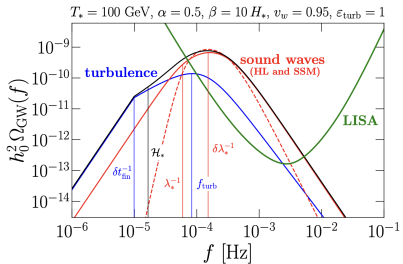
$$f_* \simeq 1.64 \times 10^{-3} \frac{100}{R_* \mathcal{H}_*} \frac{T_*}{100 \text{ GeV}} \text{ Hz}$$

- Phase transitions
  - Ground-based detectors (LVK, ET, CE) frequencies are 10–1000 Hz  
Peccei-Quinn, B-L, left-right symmetries  $\sim 10^7, 10^8$  GeV.
  - Space-based detectors (**LISA**) frequencies are  $10^{-5}$ – $10^{-2}$  Hz  
**Electroweak phase transition**  $\sim 100$  GeV
  - Pulsar Timing Array (PTA) frequencies are  $10^{-9}$ – $10^{-7}$  Hz  
**Quark confinement (QCD) phase transition**  $\sim 100$  MeV
- From inflation
  - $B$ -modes of CMB anisotropies ( $f_c \sim 10^{-18}$  Hz).
  - Can cover all  $f$  spectrum, depending on end-of-reheating T, and blue-tilted (beyond slow-roll inflation).

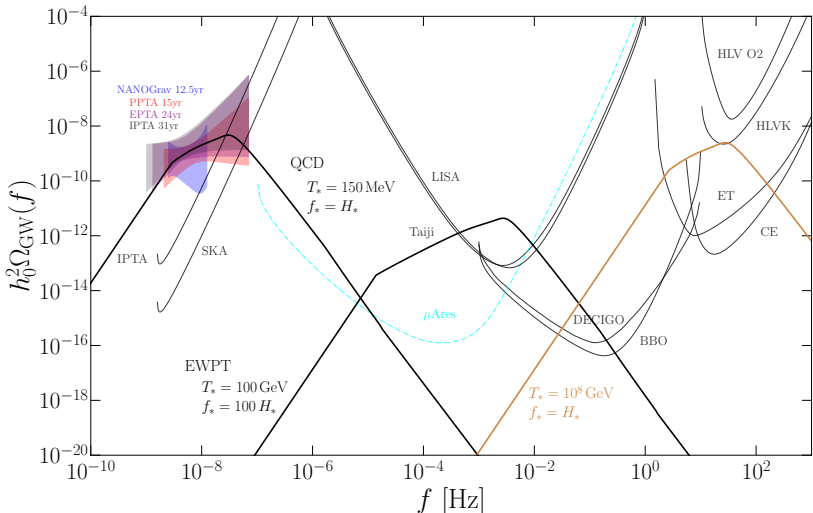
# GW sources in the early universe

- Magnetohydrodynamic (MHD) sources of GWs:
  - Sound waves generated from first-order phase transitions.
  - **Primordial magnetic fields.**
  - (M)HD turbulence from first-order phase transitions.
- High-conductivity of the early universe leads to a high-coupling between magnetic and velocity fields.
- Other sources of GWs include
  - Bubble collisions.
  - Cosmic strings.
  - Primordial black holes.
  - Inflation.

ARP *et al.*, 2307.10744, 2308.12943



## Gravitational spectrum (turbulence from PTs)<sup>6</sup>



<sup>6</sup>ARP, C. Caprini, A. Neronov, D. Semikoz, *PRD* **105**, 123502 (2022)

A. Neronov, ARP, C. Caprini, D. Semikoz, *PRD* **103**, L041302 (2021)

ARP et al., arXiv:2307.10744 (2023).

# Primordial magnetic fields

- Magnetic fields can either be produced at or present during cosmological phase transitions.
- The magnetic fields are strongly coupled to the primordial plasma and inevitably lead to MHD turbulence.<sup>7</sup>
- Present magnetic fields can be amplified by primordial turbulence via dynamo.<sup>8</sup>
- Primordial magnetic fields are assumed to reach equipartition after the phase transition, modelled as a fraction  $\varepsilon/2$  of the total energy.<sup>9</sup>

---

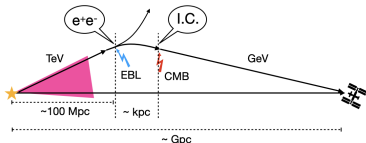
<sup>7</sup> J. Ahonen and K. Enqvist, *Phys. Lett. B* **382**, 40 (1996).

<sup>8</sup> A. Brandenburg *et al.* (incl. ARP), *Phys. Rev. Fluids* **4**, 024608 (2019).

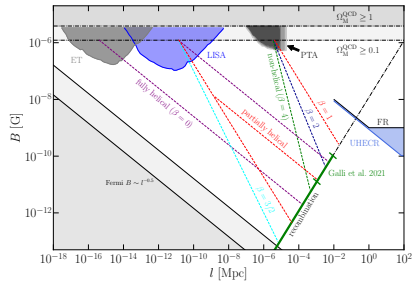
<sup>9</sup> ARP *et al.*, arXiv:2307.10744 (2023)  
[LISA Cosmology Working Group] (incl. ARP), arXiv:2403.03723 (2024)

# Multi-messenger constraints on primordial magnetic fields<sup>3</sup>

- Primordial magnetic fields would evolve through the history of the universe up to the present time and could explain the lower bounds in cosmic voids found by the Fermi collaboration.<sup>4</sup>



- Maximum amplitude of primordial magnetic fields is constrained by the big bang nucleosynthesis.<sup>5</sup>
- Additional constraints from CMB, Faraday Rotation, ultra-high energy cosmic rays (UHECR).



- CTA telescopes will allow to explore a broader range of parameters of the intergalactic magnetic field with strengths 1–10 pG, estimated<sup>6</sup> using deep exposure of the nearest hard spectrum blazar Mrk 501

<sup>3</sup> ARP *et al.*, arXiv:2307.10744 (2023).

<sup>4</sup> A. Neronov and I. Vovk, *Science* **328**, 73 (2010).

<sup>5</sup> V. F. Shvartsman, *Pisma Zh. Eksp. Teor. Fiz.* **9**, 315 (1969).

<sup>6</sup> Korochkin, Kalashev, Neronov, Semikoz, *PoS ICRC2021* (2021) 919

# Conclusions

- Primordial magnetic fields in the early universe can significantly contribute to the stochastic GW background (SGWB) and lead to the production of MHD turbulence.
- The SGWB produced by MHD turbulence requires, in general, performing high-resolution numerical simulations, which can be done using the PENCIL CODE.
- LISA, PTA (SKA), and next-generation ground-based detectors can be used to probe the origin of magnetic fields in the largest scales of our Universe, which is still an open question in cosmology.
- $\gamma$ -ray observations (Fermi LAT, CTA) can constrain intergalactic magnetic fields.
- Primordial magnetic fields can be studied in a multi-messenger approach, combining GW (interferometers and radio telescopes), CMB, and  $\gamma$ -ray observations.



# Thank You!



[alberto.roperpol@unige.ch](mailto:alberto.roperpol@unige.ch)

[github.com/AlbertoRoper/cosmoGW](https://github.com/AlbertoRoper/cosmoGW)  
[cosmology.unige.ch/users/alberto-roper-pol](https://cosmology.unige.ch/users/alberto-roper-pol)



# Extra slides

# Generation of primordial magnetic fields

- Bubble collisions and velocity fields induced by first-order phase transitions can amplify seed magnetic fields.
- Parity-violating processes during the EWPT are predicted by SM extensions that account for baryogenesis and can produce helical magnetic fields through sphaleron decay or B+L anomalies.<sup>10</sup>

$$\mathbf{B} = \nabla \times \mathbf{A} - i \frac{2 \sin \theta_w}{gv^2} \nabla \Phi^\dagger \times \nabla \Phi$$

- Axion fields can amplify and produce magnetic field helicity.<sup>11</sup>

$$\mathcal{L} \supset \frac{\phi}{f} F_{\mu\nu} \tilde{F}^{\mu\nu}$$

---

<sup>10</sup> T. Vachaspati, *Phys. Rev. B* **265**, 258 (1991), T. Vachaspati, *Phys. Rev. Lett.* **87**, 251302 (2001), J. M. Cornwall, *Phys. Rev. D* **56**, 6146 (1997).

<sup>11</sup> M. M. Forbes and A. R. Zhitnitsky, *Phys. Rev. Lett.* **85**, 5268 (2000).

# Generation of primordial magnetic fields

- Inhomogeneities in the Higgs field in low-scale electroweak hybrid inflation.<sup>12</sup>
- Magnetic fields from inflation can be present during phase transitions (non-helical<sup>13</sup> and helical<sup>14</sup>).
- Low-scale (QCD and EWPT) magnetogenesis during reheating.<sup>15</sup>
- Chiral magnetic effect.<sup>16</sup>

---

<sup>12</sup> M. Joyce and M. E. Shaposhnikov, *Phys. Rev. Lett.* **79**, 1193 (1997), J. García-Bellido *et al.*, *Phys. Rev. D* **60**, 123504 (1999).

<sup>13</sup> M. S. Turner and L. M. Widrow, *Phys. Rev. D* **37**, 2743 (1988).

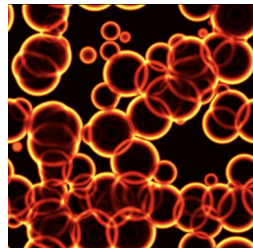
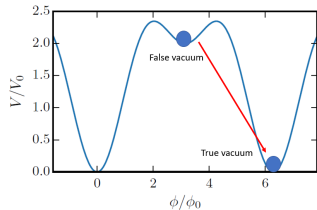
<sup>14</sup> M. Giovannini, *Phys. Rev. D* **58**, 124027 (1998).

<sup>15</sup> R. Sharma, *Phys. Rev. D* **97**, 083503 (2018).

<sup>16</sup> M. Joyce and M. E. Shaposhnikov, *PRL* **79**, 1193 (1997).

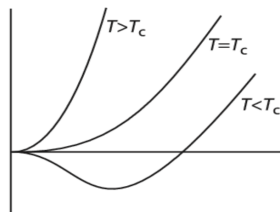
# First-order phase transition

$$V(\phi, T) = \frac{1}{2}M^2(T)\phi^2 - \frac{1}{3}\delta(T)\phi^3 + \frac{1}{4}\lambda\phi^4$$

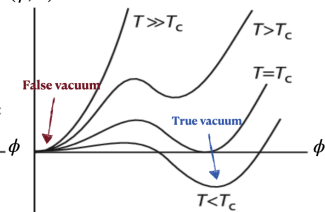


Credits: I. Stomberg

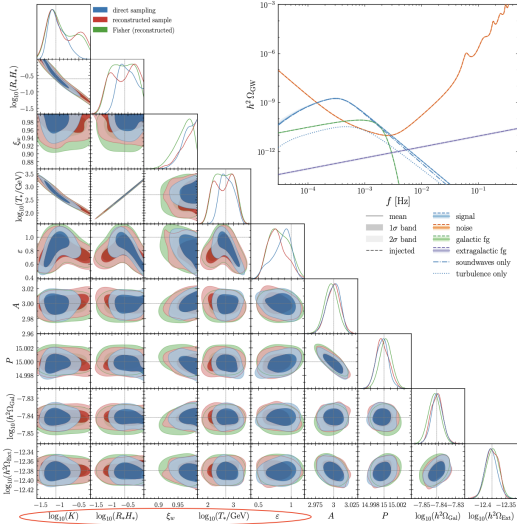
$V(\phi, T)$       **2nd order**



$V(\phi, T)$       **1st order**



# Parameter reconstruction of phase transitions with LISA<sup>17</sup>



$K$ : fraction of kinetic energy density

$R_*$ : mean size of bubbles

$\xi_w$ : velocity of bubbles

$T_*$ : temperature at the end of the PT

$\epsilon$ : fraction of turbulence energy density

# GWs from (M)HD turbulence

- Direct numerical simulations using the PENCIL CODE<sup>18</sup> to solve:
  - ① Relativistic MHD equations adapted for radiation-dominated era (after electroweak symmetry is broken).
  - ② Gravitational waves equation.
- In general, large-resolution simulations are necessary to solve the MHD nonlinearities (e.g., unequal-time correlators UETC and non-Gaussianities, which require simplifying assumptions in analytical studies).

<sup>18</sup>

Pencil Code Collaboration, JOSS **6**, 2807 (2020), <https://github.com/pencil-code/ARP> et al., Geophys. Astrophys. Fluid Dyn. **114**, 130 (2020).

## Conservation laws for MHD turbulence

$$T^{\mu\nu}_{;\nu} = 0, \quad F^{\mu\nu}_{;\nu} = -J^\mu, \quad \tilde{F}^{\mu\nu}_{;\nu} = 0$$

In the limit of subrelativistic bulk flow:

$$\gamma^2 \sim 1 + (\nu/c)^2 + \mathcal{O}(\nu/c)^4$$

Relativistic MHD equations are reduced to<sup>19</sup>

$$\frac{\partial \ln \rho}{\partial t} = -\frac{4}{3} (\nabla \cdot \mathbf{u} + \mathbf{u} \cdot \nabla \ln \rho) + \frac{1}{\rho} [\mathbf{u} \cdot (\mathbf{J} \times \mathbf{B}) + \eta \mathbf{J}^2],$$

$$\frac{D\mathbf{u}}{Dt} = \frac{1}{3} \mathbf{u} (\nabla \cdot \mathbf{u} + \mathbf{u} \cdot \nabla \ln \rho) - \frac{\mathbf{u}}{\rho} [\mathbf{u} \cdot (\mathbf{J} \times \mathbf{B}) + \eta \mathbf{J}^2]$$

$$-\frac{1}{4} \nabla \ln \rho + \frac{3}{4\rho} \mathbf{J} \times \mathbf{B} + \frac{2}{\rho} \nabla \cdot (\rho \nu \mathbf{S}),$$

$$\frac{\partial \mathbf{B}}{\partial t} = \nabla \times (\mathbf{u} \times \mathbf{B} - \eta \mathbf{J}), \quad \mathbf{J} = \nabla \times \mathbf{B},$$

for a flat expanding universe with comoving and normalized

$\mathbf{p} = a^4 \mathbf{p}_{\text{phys}}$ ,  $\rho = a^4 \rho_{\text{phys}}$ ,  $B_i = a^2 B_{i,\text{phys}}$ ,  $u_i$ , and conformal time  $t$  ( $dt = a dt_c$ ).

<sup>19</sup>

A. Brandenburg, et al., Phys. Rev. D **54**, 1291 (1996).

## GW equation for a flat expanding Universe

- Assumptions: isotropic and homogeneous Universe.
- Friedmann–Lemaître–Robertson–Walker (FLRW) metric  $\gamma_{ij} = a^2 \delta_{ij}$ .
- Tensor-mode perturbations above the FLRW model:

$$g_{ij} = a^2 \left( \delta_{ij} + h_{ij}^{\text{phys}} \right), \quad |h_{ij}^{\text{phys}}| \ll |g_{ij}|$$

- GW equation is<sup>20</sup>

$$\left( \partial_t^2 - \frac{a''}{a} - c^2 \nabla^2 \right) h_{ij} = \frac{16\pi G}{a c^2} T_{ij}^{\text{TT}}$$

- $h_{ij}$  are rescaled  $h_{ij} = a h_{ij}^{\text{phys}}$ .
- Comoving spatial coordinates  $\nabla = a \nabla^{\text{phys}}$ .
- Conformal time  $dt = a dt_c$ .
- Comoving stress-energy tensor components  $T_{ij} = a^4 T_{ij}^{\text{phys}}$ .
- Radiation-dominated epoch such that  $a'' = 0$ .

<sup>20</sup>L. P. Grishchuk, Sov. Phys. JETP 40, 409 (1974).

# Numerical results for decaying MHD turbulence<sup>21</sup>

## Initial conditions

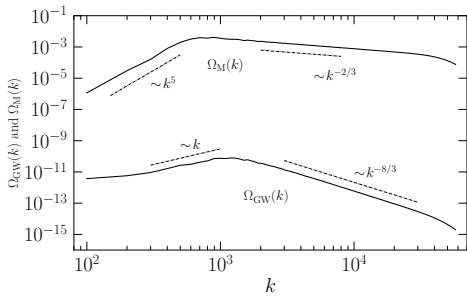
- Initial stochastic magnetic (or velocity) field with fractional helicity  $\sigma_M$ .  
$$kB_i(\mathbf{k}) = \left( \delta_{ij} - \hat{k}_i \hat{k}_j - i\sigma_M \epsilon_{ijl} \hat{k}_l \right) g_j \sqrt{2\Omega_M(k)/k}$$
- Batchelor spectrum for magnetic (or vortical velocity) fields, i.e.,  $\Omega_M \propto k^5$  for small  $k < k_* \sim \mathcal{O}(\xi_M^{-1})$ .
- Kolmogorov spectrum in the inertial range, i.e.,  $\Omega_M \propto k^{-2/3}$ .

---

<sup>21</sup>A. Brandenburg *et al.* (incl. ARP), *Phys. Rev. D* **96**, 123528 (2017).  
ARP *et al.*, *Phys. Rev. D* **102**, 083512 (2020).  
ARP *et al.*, *JCAP* **04** (2022), 019.  
ARP *et al.*, *Phys. Rev. D* **105**, 123502 (2022).

## Numerical results for decaying MHD turbulence<sup>22</sup>

$$1152^3, k_* = 2\pi \times 100, \Omega_M \sim 10^{-2}, \sigma_M = 1$$



- **Characteristic  $k$  scaling in the subinertial range for the GW spectrum.**
- $k^2$  expected at scales  $k < k_*$  and  $k^3$  at  $k < H_*$  according to the “top-hat” model (Caprini *et al.*, 2020).

<sup>22</sup>ARP *et al.*, Phys. Rev. D 102, 083512 (2020).

## Analytical model for GWs from decaying turbulence

- Assumption: magnetic or velocity field evolution  $\delta t_e \sim 1/(u_* k_*)$  is slow compared to the GW dynamics ( $\delta t_{\text{GW}} \sim 1/k$ ) at all  $k \gtrsim u_* k_*$ .
- We can derive an analytical expression for nonhelical fields of the envelope of the oscillations<sup>23</sup> of  $\Omega_{\text{GW}}(k)$ .

$$\Omega_{\text{GW}}(k, t_{\text{fin}}) \approx 3 \left( \frac{k}{k_*} \right)^3 \Omega_M^* {}^2 \frac{\mathcal{C}(\alpha)}{\mathcal{A}^2(\alpha)} p_\Pi \left( \frac{k}{k_*} \right) \\ \times \begin{cases} \ln^2[1 + \mathcal{H}_* \delta t_{\text{fin}}] & \text{if } k \delta t_{\text{fin}} < 1, \\ \ln^2[1 + (k/\mathcal{H}_*)^{-1}] & \text{if } k \delta t_{\text{fin}} \geq 1. \end{cases}$$

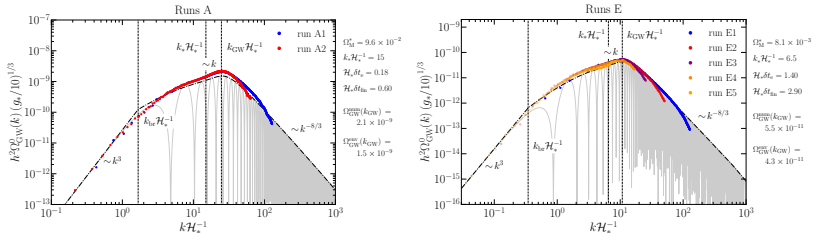
- $p_\Pi$  is the anisotropic stress spectrum and depends on spectral shape, can be approximated for a von Kármán spectrum as<sup>24</sup>

$$p_\Pi(k/k_*) \simeq \left[ 1 + \left( \frac{k}{2.2k_*} \right)^{2.15} \right]^{-11/(3 \times 2.15)}$$

<sup>23</sup>ARP *et al.*, Phys. Rev. D **105**, 123502 (2022).

<sup>24</sup>ARP *et al.*, arXiv:2307.10744 (2023).

# Numerical results for nonhelical decaying MHD turbulence<sup>25</sup>



run	$\Omega_M^*$	$k_* \mathcal{H}_*^{-1}$	$\mathcal{H}_* \delta t_e$	$\mathcal{H}_* \delta t_{\text{fin}}$	$\Omega_{\text{GW}}^{\text{num}}(k_{\text{GW}})$	$[\Omega_{\text{GW}}^{\text{env}}/\Omega_{\text{GW}}^{\text{num}}](k_{\text{GW}})$	$n$	$\mathcal{H}_* L$	$\mathcal{H}_* t_{\text{end}}$	$\mathcal{H}_* \eta$
A1	$9.6 \times 10^{-2}$	15	0.176	0.60	$2.1 \times 10^{-9}$	1.357	768	$6\pi$	9	$10^{-7}$
A2	—	—	—	—	—	—	768	$12\pi$	9	$10^{-6}$
E1	$8.1 \times 10^{-3}$	6.5	1.398	2.90	$5.5 \times 10^{-11}$	1.184	512	$4\pi$	8	$10^{-7}$
E2	—	—	—	—	—	—	512	$10\pi$	18	$10^{-7}$
E3	—	—	—	—	—	—	512	$20\pi$	61	$10^{-7}$
E4	—	—	—	—	—	—	512	$30\pi$	114	$10^{-7}$
E5	—	—	—	—	—	—	512	$60\pi$	234	$10^{-7}$

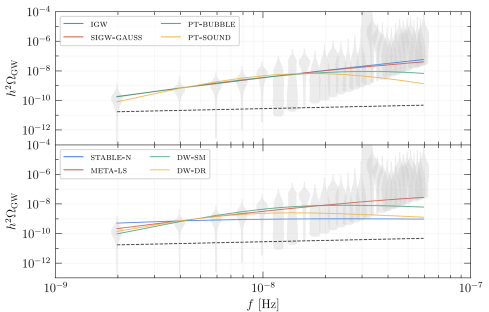
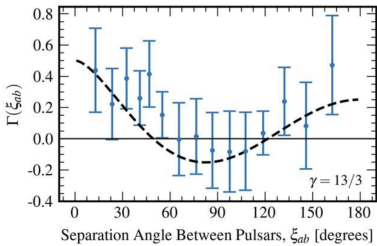
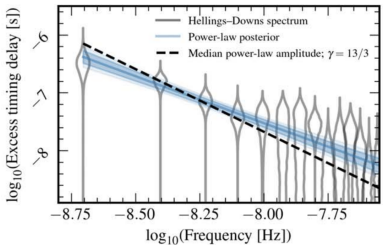
<sup>25</sup> ARP et al., Phys. Rev. D 105, 123502 (2022).

# Pulsar Timing Array (PTA) collaborations

- International PTA collaborations combine their data in the IPTA collaboration.
- European Pulsar Timing Array (EPTA): *Effelsberg, Lovell, Nançay Radio Telescope, Sardinia Radio Telescope, Westerbork Synthesis Radio Telescope.*
- North American Nano-Hertz Observatory for Gravitational Waves (NANOGrav): *Green Bank Telescope (GBT), Arecibo (until 2020), Very Large Array (VLA), Canadian Hydrogen Intensity Mapping Experiment (CHIME).*
- Parkes PTA (PPTA): *Murriyang radio telescope.*
- Indian PTA (InPTA): *GMRT.*
- Chinese Pulsar Timing Array (CPTA): *Five-hundred-meter Aperture Spherical Telescope (FAST).*
- MeerKAT PTA (MPTA).

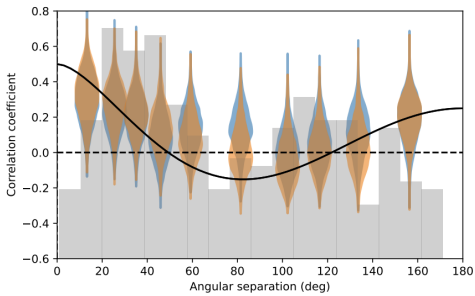
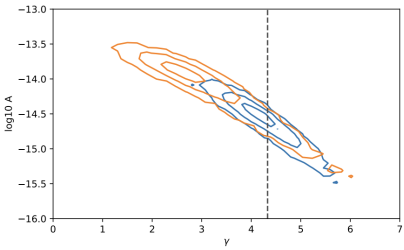
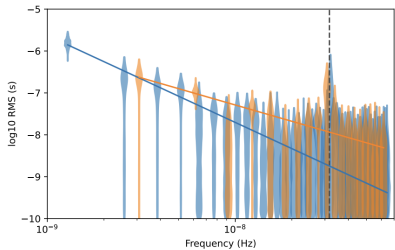


## NANOGrav 15 yr data observation<sup>26</sup>



<sup>26</sup>[NANOGrav collaboration], *ApJ Lett.* **951**, 8 & 11 (2023).

# EPTA 24.7 yr data observation (DR 2)<sup>27</sup>



<sup>27</sup>[EPTA Collaboration], arXiv:2306.16224.

# Primordial magnetic fields constraints with EPTA DR 2<sup>28</sup>

